JOURNAL OF MATERIALS SCIENCE 28 (1993) 6066–6069

Electron microscopic observation of rapidly cooled ZrO_2–3 mol% Sm_2O_3 from the melt

M. HAYAKAWA, Y. ONDA*, M. OKA
Department of Mechanical Engineering, Tottori University, Koyama, Tottori 680, Japan
M. YOSHIMURA, M. YASHIMA
Research Laboratory of Engineering Materials, Tokyo Institute of Technology, 4259, Nagatsuta, Midori, Yokohama 227, Japan

Electron microscopic observation was made on ZrO_2–3 mol% Sm_2O_3 specimens prepared from the melt using two different cooling rates, namely rapid quenching using a hammer–anvil apparatus and free cooling on a water-cooled copper hearth. The observed microscopic features, such as fully tetragonal grains with parallel twins or herringbone structure, anti-phase boundary contrast in a dark-field image, tweed structure, etc., were found to be quite similar to those observed in similarly prepared ZrO_2–3 mol% Y_2O_3 specimens. It was specifically noted that the tweed structure, which requires atomic diffusion, was not suppressed by the rapid quenching, indicating a very fast growth rate. Trace analysis was also conducted on the tweed structure observed in freely cooled specimens.

1. Introduction

The high-temperature phases with cubic and tetragonal symmetries of zirconia can be partially or fully stabilized at room temperature by adding various kinds of metals oxides resulting in very useful properties of practical use (see, for example, [1]). Although MgO, CaO, and Y_2O_3 have been traditionally used as stabilizing oxides in commercial materials, several other oxides are also known to serve as successful stabilizers. Thus the influence of various oxides on the phase limit and the stability is of great interest.

Recently, Yoshimura *et al.* [2] studied the phase relations in a series of ZrO_2–R_2O_3 (R = Nd, Sm, Er, Yb, and Sc) prepared by rapid quenching from the melt, and compared the results with the existing data for the ZrO_2–Y_2O_3 system. The main conclusions were: (1) the existing region of the tetragonal phase was 2–14 mol% $RO_{1.5}$ regardless of the dopant species; (2) the lattice parameters of the tetragonal and cubic phases varied linearly with the amount of dopant, and the increment of the cube root of unit cell volume for a fixed composition was linear with the ionic radii of the dopants; (3) the c/a ratio of the tetragonal phase was dependent on the content of the dopant but almost independent of the species.

They also showed several electron micrographs of ZrO_2–8 mol% $ErO_{1.5}$, which were suggestive of similarity to the ZrO_2–Y_2O_3 system. In the ZrO_2–Y_2O_3 system, particularly in arc-melted specimens, a variety of microstructures has been found with varying compositions and heat treatments. Because the evolution of microstructures is a direct consequence of phase transformation, much discussion has been devoted to the interpretation of the microstructure in conjunction with the transformation mechanism.

Although a complete agreement has not been reached on the transformation mode of the ZrO_2–Y_2O_3 system, it is also of interest to investigate the microstructure of other ZrO_2–R_2O_3 systems. The objective of the present work was to study the microstructure of a ZrO_2–3 mol% Sm_2O_3 alloy prepared from the melt with different cooling rates and to compare the results with those of the ZrO_2–Y_2O_3 system.

2. Experimental procedures

High-purity ZrO_2 (99.9%, Soekawa Rikagaku Co. Ltd, Tokyo, Japan) and Sm_2O_3 (99.9%, Shinetu Chemical Co. Ltd, Tokyo, Japan) were weighed to make ZrO_2–6 mol% $SmO_{1.5}$, hereafter denoted 3% Sm_2O_3. The powders were mixed in an agate mortar with methanol and pressed into pellets 3 mm high and 2 mm diameter. Two different methods of melting and cooling procedures were used. In one method, a pellet was melted in air using a xenon arc-image furnace and then rapidly quenched with a copper-made hammer–anvil apparatus. Films about 20 μm thick were obtained; the cooling rate was estimated to be higher than 10^5 K s^{-1} [3]. In the other method, several beads were placed together on a water-cooled copper hearth and re-melted by argon plasma arc. The melt was freely cooled on the copper hearth after shutting off the arc; the specimen took 2 s to cool to 1500 °C and 10 s to 1000 °C. Specimens prepared by these two methods are referred to as rapidly quenched specimens and freely cooled specimens, respectively.

* *Present address*: Hitachi Metals Co. Ltd, Chiyoda, Tokyo 100, Japan.

0022–2461

Films of rapidly quenched specimens were directly subjected to ion-beam thinning, whereas freely cooled specimens were sliced and mechanically ground to about 20 μm thickness before ion-beam thinning. These specimens were carbon coated and examined under the transmission electron microscope (JEM 200A, Jeol, Tokyo, Japan) operated at 200 kV.

3. Results

3.1. Rapidly quenched specimen

Typical microstructure of a rapidly quenched specimen is shown in Fig. 1a and b. Grains were fairly uniform and were about 2 μm in size. They were often occupied by more or less regularly spaced twin lamellae (a) or subdivided into twinned patches (b). The latter structure resembles the herringbone structure of an arc-melted ZrO_2–Y_2O_3 alloy. In either structure the twin spacing was about 100 nm. When a dark-field image was taken through a (1 1 2) type diffraction spot, anti-phase boundary (APB) contrast was revealed (Fig. 2). The domain size was estimated to be 50 nm or less. The above result indicates that the tetragonal phase of the present alloy is of Teufer structure [4] which is characterized by anion displacement along the *c*-axis. All of the above described features had been observed in rapidly quenched 3% Y_2O_3 specimens [3] and the structures were identical in all practical interest.

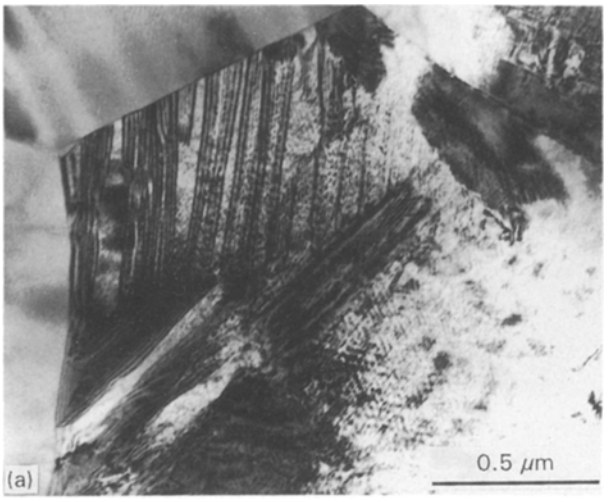

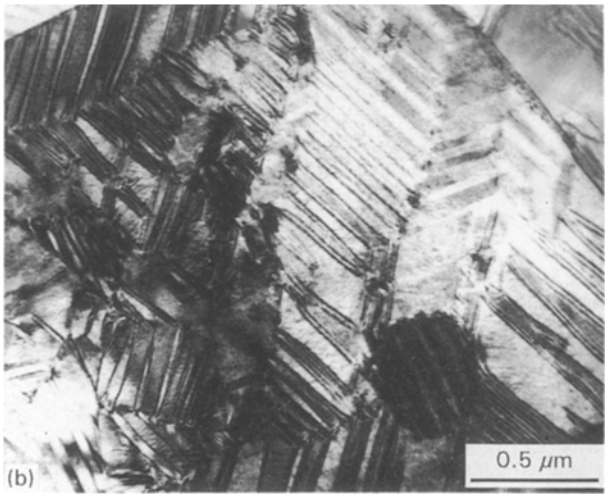

Figure 1 Electron micrographs of rapidly quenched specimens showing representative grains occupied by (a) parallel twins and (b) twinned patches.

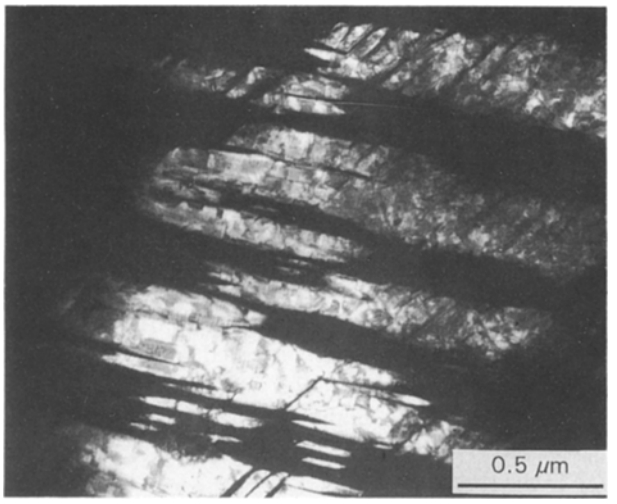

Figure 2 Dark-field image of a rapidly quenched specimen taken through the (1 1 2) diffraction spot. APB contrast is visible in the diffracting twin variants.

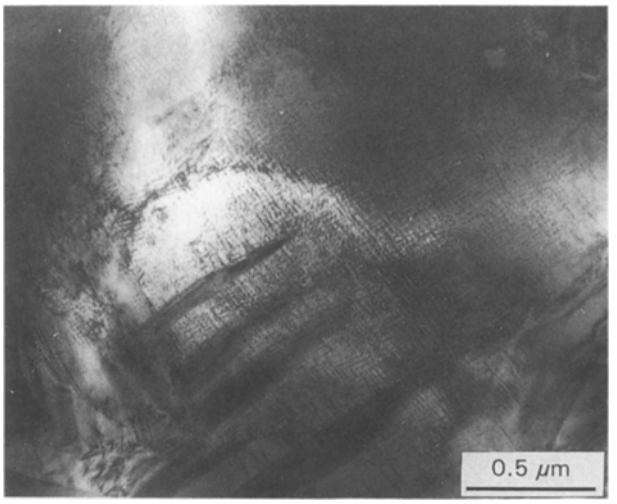

Figure 3 Electron micrograph of a rapidly quenched specimen showing tweed structure.

An interesting feature is the tweed structure as shown in Fig. 3. The fine contrast normally appears in two directions with 20 nm spacing and exhibits basket-woven structure. The structures were practically the same as those observed in an arc melted ZrO_2–Y_2O_3 specimen [5–7]. Because the tweed structure is considered to form by a diffusional process, the reaction rate must be quite high so as not to have been suppressed by the cooling rate employed here. Although the tweed structure has not been specifically mentioned in the previous paper on ZrO_2–Y_2O_3 specimens, a somewhat similar contrast can be seen in Fig. 2c of [3]. Thus the fast formation of the tweed structure in a rapidly quenched specimen should not be taken as a unique feature of the present system.

3.2. Freely cooled specimen

Fig. 4 shows a typical structure of a specimen freely cooled from the melt. It is characterized by a well-developed herringbone structure, as often reported in

a similarly prepared 3% Y_2O_3 specimen [8, 9]. The structure comprises alternation of two types of bands lying along (1 1 0) planes and each type of band contains (1 0 1) twins. A complete annihilation of the shear strain associated with the c-t′ transformation is achieved when the twin ratio in each band is 2. The twin spacing was about 200 nm, which was somewhat larger than in a rapidly quenched specimen but roughly the same as in a freely cooled ZrO_2–Y_2O_3 specimen. The tweed structure could be more clearly observed than in a rapidly quenched specimen. It also appears to be the same as those observed in an arc-melted ZrO_2–Y_2O_3, for which two of the present authors identified the habit plane was on $\{2\,2\,3\}_t$ planes [7]. However, $\{1\,0\,1\}$ and $\{1\,1\,1\}$ planes have been reported by other workers [6, 10].

Trace analysis was conducted and an example is shown in Fig. 5. As demonstrated in a previous paper [7], the coexistence of the herringbone structure provides a convenient means of identifying the habit plane indices of the tweed structure in the tetragonal basis. This is because once the twin planes and the band boundary are indexed, the *c*-axis of the twin variants in each band can be uniquely identified. In the structure of Fig. 5a, for example, the thicker variants in A and B bands are *x* and *y* variants, respectively, namely the *c*-axis of these variants are along *x* and *y* directions in the reference coordinate system to which the indices of the herringbone structure are referred. Assuming that the tweed structure had developed in the course of the decomposition of the t′ (diffusionlessly formed tetragonal phase) into the equilibrium t and c phases, an ellipsoidal inclusion method using anisotropic elasticity [11] predicted a $(2\,2\,3)_t$ habit, thus (3 2 2) and (2 3 2) for *x* and *y* variants, respectively.

The trace directions could be read on the micrograph only with a certain angular range because of the wavy nature of the tweed contrast. These angular ranges are shown by thick arcs, T_1–T_4, along the larger circle (S) representing the foil surface of Fig. 5a, and the corresponding ranges of trace normals by L_1–L_4. It is seen that the ranges of trace normals, L1 and L2, which are related to the *y* variant, include $2\,\bar{3}\,2$ and $2\,3\,2$ poles, respectively, whereas L3 and L4, which are related to the *x* variant, include $\bar{3}\,2\,2$ and $3\,2\,2$ poles, respectively. Thus, the observed traces are consistent with the predicted habit planes of (2 3 2) type. However, in this example, the observed trace directions are also consistent with the (1 1 1) or (1 0 1) habit. We worked out three other micrographs, but the results left similar ambiguity, although a better overall agreement was obtained for the (2 2 3) type habit than others.

Fig. 6 shows another example of the tweed structure, which appeared in a region free from the herringbone structure. In this tweed structure the contrast was fuzzy and a basket-woven structure could no

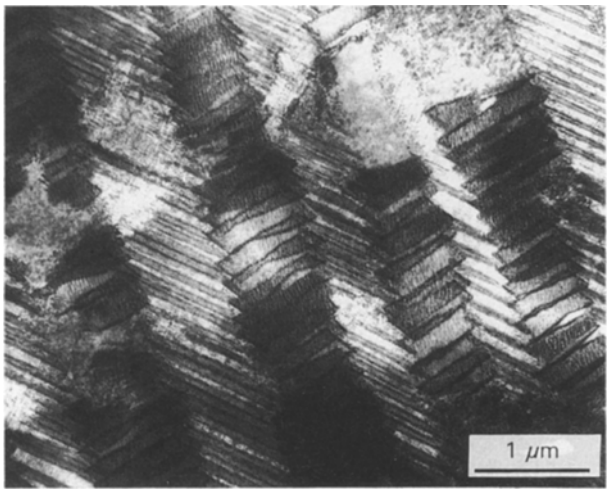

Figure 4 Electron micrograph of a freely cooled specimen showing a well-defined herringbone structure.

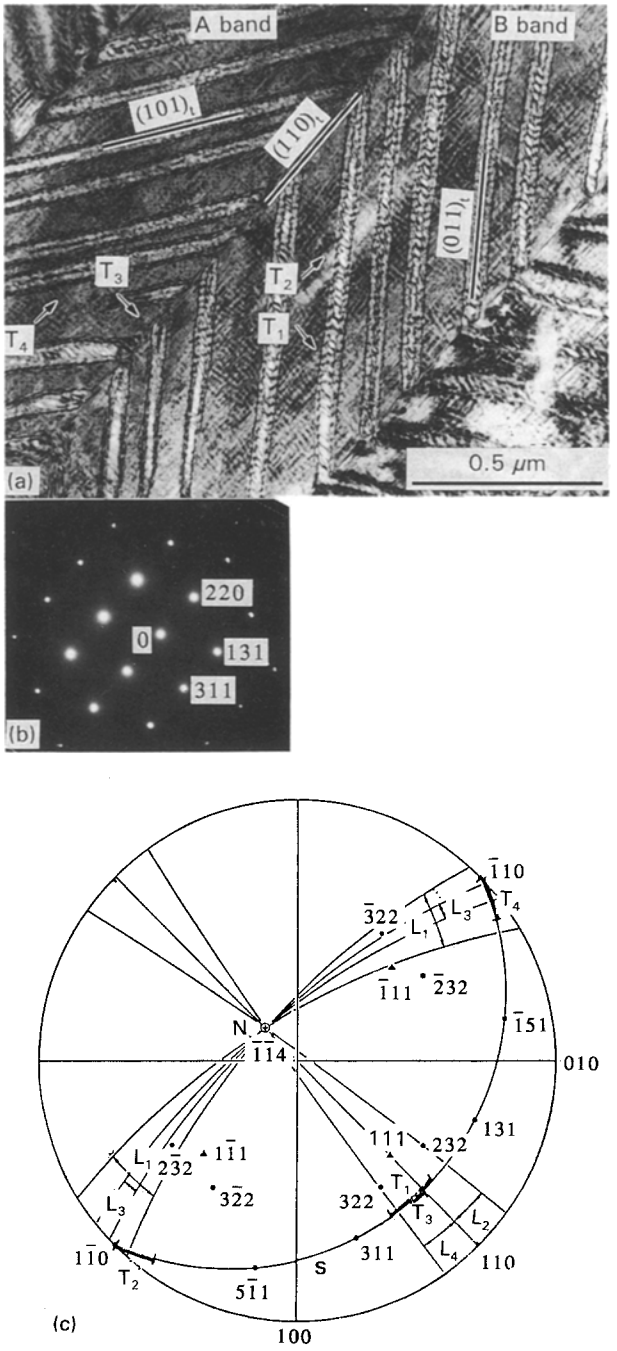

Figure 5 (a) Electron micrograph of a freely cooled specimen showing a tweed structure along with the herringbone structure. (b) Diffraction pattern. (c) Stereoprojection of trace directions, T_1–T_4, and corresponding trace normals, L_1–L_4. The traces were most consistent with $\{2\,2\,3\}$ habit planes.

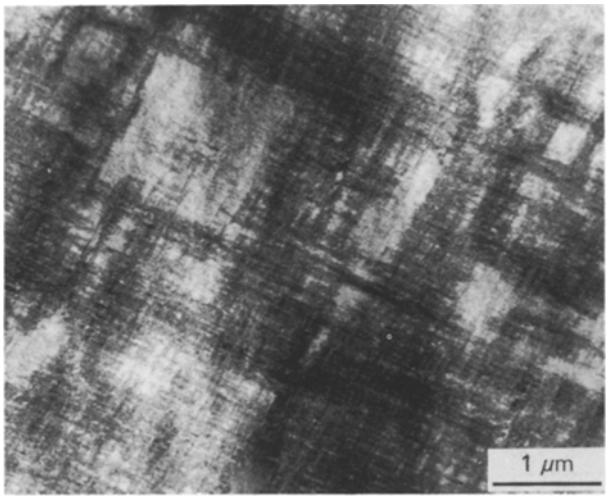

Figure 6 Electron micrograph of the tweed contrast which appeared in a region free from a herringbone structure. The contrast is fuzzier and basket-woven structure is no longer resolved.

longer be resolved. The absence of the herringbone structure may indicate somewhat higher solute content in these regions. In the ZrO_2–Y_2O_3 system, for example, the herringbone structure is ubiquitously present in 3 mol % but they are absent in 4 mol %. A slight compositional fluctuation may occur in a freely cooled specimen. Therefore, these tweed structures would have been formed at lower temperature than the previously observed one and this may represent an earlier stage of decomposition.

4. Discussion

General features of the microstructure of 3% Sm_2O_3 prepared by rapid quenching and free cooling from the melt were found to be very similar to those of 3% Y_2O_3 prepared by the same methods. This is quite reasonable in view of the previous results [2] which showed that the range of the tetragonal phase was independent of the kind of dopant and depended only on the composition. Although the present study was made only on a single composition, the similarity of the twin structures to those of Y_2O_3 of the same composition suggested a similar composition dependence as in the ZrO_2–Y_2O_3 system.

An interesting feature of the present study was the observation of tweed structure in a rapidly quenched specimen. Although this structure has not been reported in the previous paper, in view of the general resemblance, this should have been present in a rapidly quenched 3% Y_2O_3 specimen. The fast decomposition, which was insuppressible by the rapid quenching and the lower decomposition temperature for a slightly higher solute content as revealed by the finer tweed structure in the herringbone-free region, may favour spinodal decomposition, as suggested by Sakuma *et al.* [12], though this does not constitute a proof.

A habit plane orientation plays an important role in deducing the decomposition mechanism. From a purely experimental view point, however, the present trace analysis was rather inconclusive, mainly because of the waviness of the tweed structure. Nevertheless, because of the overall similarities between the present specimen and 3% Y_2O_3 specimen, we tend to believe the habit planes are also the same. At least the (2 2 3) habit has been predicted from theoretical basis . If it is possible to make the tweed structure straighter, e.g. by annealing, more precise determination may be possible.

5. Conclusion

Electron microscopic observation was made on ZrO_2–3 mol % Sm_2O_3 specimens prepared by rapid quenching or free cooling from the melt. In rapidly quenched specimens, twin lamellae and fine tweed structures were observed, whereas in freely cooled specimens, twins were mostly arranged in a herringbone structure and the tweed structure became coarser and clearer. These structures were very similar to those observed in similarly prepared ZrO_2–3 mol % Y_2O_3 specimens. The habit planes of the tweed structure could not be determined accurately, because of the waviness of the traces, but appeared to lie somewhere near (2 2 3)–(1 1 1).

References

1. A. H. HEUER and L. W. HOBBS (eds), "Science and Technology of Zirconia", Advances in Ceramics, Vol. 3 (American Ceramic Society, Columbus, OH, 1981).
2. M. YOSHIMURA, M. YASHIMA, T. NOMA and S. SŌMIYA, *J. Mater. Sci.* **25** (1990) 2011.
3. T. NOMA, M. YOSHIMURA, M. KATO, M. SHIBATA, H. SETO and S. SŌMIYA, *Yogyo-Kyokai-Shi* (*J. Ceram. Soc. Jpn*) **94** (1986) 887.
4. G. TEUFER, *Acta Crystallogr* **15** (1962) 1187.
5. R. CHAIM, M. RÜHLE and A. H. HEUER, *J. Am. Ceram. Soc.* **68** (1985) 427.
6. T. SAKUMA, Y. YOSHIZAWA and H. SUTO, *J. Mater. Sci.* **20** (1985) 1085.
7. M. HAYAKAWA, K. ADACHI and M. OKA. *Acta. Metall. Mater.* **38** (1990) 1761.
8. T. SAKUMA, Y. YOSHIZAWA and H. SUTO, *J. Mater. Sci.* **20** (1985) 2399.
9. M. HAYAKAWA, M. TADA, H. OKAMOTO and M. OKA, *Trans. Jpn Inst. Metals* **27** (1986) 750.
10. R. H. J. HANNINK, *J. Mater. Sci.* **13** (1978) 2487.
11. T. MURA and T. MORI, "Micromechanics" (Baifukan, Tokyo, 1976) Ch. 3.
12. T. SAKUMA, Y. YOSHIZAWA and H. SUTO, *J. Mater. Sci.* **21** (1986) 1436.

Received 23 June 1992
and accepted 20 April 1993